The International Journal of Advanced Manufacturing Technology (2018) 95:1989–2003
https://doi.org/10.1007/s00170-017-1403-x

ORIGINAL ARTICLE

Prediction of friction stir weld quality without and with signal features

D. J. Huggett[1] · T. W. Liao[1] · M. A. Wahab[1] · A. Okeil[2]

Received: 25 October 2017 / Accepted: 13 November 2017 / Published online: 17 November 2017

Abstract
Building a reliable prediction model can mitigate the need for actual experiments, hence saving time and cost. To this end, this study presents a methodology to predict weld quality for a particular friction stir weld configuration using machine learning and metaheuristic algorithms including K-nearest neighbor (KNN), fuzzy KNN (FKNN), and the artificial bee colony (ABC). The ABC algorithm was utilized to determine the best (F)KNN model with optimal *K* value and feature subset. First, models were built based on only experimental conditions including spindle rotational speed, plunge force, and feed rate, as well as derived values including a speed ratio and an empirical force index (EFI). The best model was identified to be 1-NN comprised of three features, i.e., rotational speed, feed rate, and EFI, with 93.16% classification accuracy based on leave-one-out cross-validation. The majority of data points leading to error were found to lie mostly on the boundaries between classes. It was shown that classification error could be reduced by removing those points, which is cheating and not recommended. Instead, it is recommended to improve classification accuracy without omitting dissenting data by introducing additional information to better distinguish misclassified data points. To this end, wavelet energy features extracted from weld signals of X-Force, Y-Force, spindle rotational speed, feed rate, and plunge force were added to the original feature pool. In order to determine the impact of each weld signal feature set, each signal feature set was individually tested. After applying ABC to the expanded feature pool to build the best model, perfect classification accuracy was achieved in several cases. The results suggest that adding signal features can greatly improve the effectiveness of model predictability of friction stir weld quality.

Keywords Friction stir welding · Artificial bee colony · K-nearest neighbor · Weld quality classification · Welding process signals

1 Introduction

The solid-state, thermomechanical, grain refining, plastic deformation process of friction stir welding (FSW) has been the subject of extensive research in the past three decades. FSW has proven to obtain high-strength joints for aluminum alloys [1] and has also illustrated to be successful in joining steel and other non-conventional alloys [2, 3]. Obtaining quality FSW joints often relies on the experience of the operator/engineer who is knowledgeable of the process. Such experience is valuable but not always accessible because of its proprietary nature. In the case where process parameter combinations for defect-free welds are unknown, trial-and-error experimentation is often conducted. To minimize the time and cost needed to carry out actual experiments, efforts have been made by researchers to build reliable prediction models of weld quality that can be analytical, numerical, or data-driven in nature.

Analytical modeling utilizes physical principles to find a solution and has been utilized for the FSW process as seen in refs. [4–7]. Numerical models aim to approximate solutions by iterating through a time-stepping procedure as observed in refs. [8, 9]. Data-driven models fall under the realm of informatics, which is based upon computational intelligence and machine learning algorithms [10]. Here, computational intelligence routines create connections between input (experimental data) and output behavior without the need to know the physical behavior of the system. In this study, the data-driven modeling approach is followed for prediction of weld quality for friction stir welds by employing FSW critical process parameters, a pin speed ratio, weld signal features, and an empirical relation as input features. The reason for focusing on the data-driven modeling approach is that, to the best of our knowledge, no analytical or numerical models exist today capable of predicting weld flaws for various processing conditions during FSW.

✉ M. A. Wahab
wahab@me.lsu.edu

[1] Department of Mechanical and Industrial Engineering, Louisiana State University, Baton Rouge, LA 70803, USA

[2] Department of Civil and Environmental Engineering, Louisiana State University, Baton Rouge, LA 70803, USA

In the literature, various data-driven modeling techniques have been employed to build prediction models. It is evident these tools have become popular in the literature for weld applications as the process conditions which cause problems to weld quality can be identified [11–21]. Data-driven processes have specifically been applied to FSW. Those works are illustrated in Table 1, where identification of the study's objective, machine learning technique, input type (process parameters (PP), signal features (SF), mechanical properties (MP)), and feature extraction process (none indicates no signals used) are provided.

The works in Table 1 illustrate data-driven modeling techniques can accurately predict weld quality. In this work, the data-driven techniques of K-nearest neighbor (KNN) and fuzzy KNN (FKNN) are employed with both K-fold and leave-one-out cross-validation (LOOCV). Furthermore, the artificial bee colony (ABC) was used to provide the feature selection ability to enhance the classification techniques. The only study that has employed ABC in FSW application is [36], in which ABC was utilized to optimize fuzzy prediction models, not feature selection. Moreover, in our study, ABC is utilized not only for feature selection, but also for optimization of the K value in KNN or FKNN which to the author's knowledge is the first time this is accomplished for FSW applications.

Features of various FSW signals have been utilized for weld quality prediction as seen in Table 1. Some studies used only process parameters whereas others used only signal features. The study of Das et al. [27] is the only one that makes use of both process parameters and signal features. Our study differs from [27] in several aspects: material welded (AA-2219 vs. AA-1100), welding control method (load-control vs. position-control), signals acquired during welding (multiple vs. torque only), weld quality data (3-class vs. 2-class), model output (quality vs. tensile strength), modeling method (KNN vs. SVM), and feature selection (yes vs. no). The new contributions of this study include:

- Building weld quality model based on non-destructive and destructive test results for AA-2219
- Using ABC algorithm to find better feature subset and optimal number of nearest neighbors in order to build a better weld quality classification model
- Investigating whether various signal features can improve model classification over using process parameters only

Furthermore, this study illustrates that any one of the five individual signal types can increase model predictive capabilities by comparing models created with and without signal features.

The remaining sections are organized as follows: Section 2 describes how the data used in this study was obtained which includes the FSW experiments and signal collection details, NDT testing of welds, grouping weld quality into classes, and the methods employed for weld signal feature extraction. Section 3 describes the methodology utilized to build the classification models, and Section 4 provides results and discussions. Lastly, Section 5 concludes the work.

2 FSW experimentation, weld classes, and signal feature extraction

2.1 FSW experimental conditions

FSW data was obtained from a study where 66 varying weld schedules (a schedule refers to a combination of plunge force, feed rate, and spindle rotation speed) were conducted, see Appendix 1. The welds were completed at the National Center for Advanced Manufacturing (NCAM) utilizing friction stir welders located at NASA's Michoud Assembly Facility (MAF) in New Orleans, LA. The welders employed were I-STIR Process Development System (PDS) and I-STIR Universal Weld System (UWS). The FSW joints were all conducted with a fixed pin tool as seen in Fig. 1. The shoulder, made from H13 steel, has a 30.48 mm diameter with 0.76 mm deep counterclockwise (CCW) spiral scroll of 2.92-mm pitch. The pin is interchangeable and has an MP159 cone of 10.16 mm diameter at the shoulder with 18 TPI UNC LH threads of length 7.11 mm. The pin has a 10° taper angle. Two AA-2219-T87 panels with dimensions 609.6 mm long, 152.4 mm wide, and 8.13 mm thick were friction stir welded in a butt joint configuration with the pin tool set with a 0° lead angle and zero offset from the weld centerline.

2.2 Weld quality classification and empirical indices

After welding, welds were tested with non-destructive evaluation (NDE) and destructive techniques in order to classify the weld quality corresponding to a particular weld schedule. Commonly used NDE techniques include ultrasonic testing, phased array ultrasonic testing (PAUT), X-ray radiography, liquid dye penetration tests, eddy current testing, and magnetic particle testing. Both PAUT and X-ray radiography were used in our research project. Further details of the NDE practices involved in this work can be found in [37, 38]. After the NDE processes were completed, weld specimens were sectioned with a metal-cutting saw into tensile and macrograph coupons. Tensile coupons were destructively tested with an MTS 810 Material Test System to obtain mechanical properties. Hardness and fracture surface analysis was also conducted as reported in [22]. Optical macro- and micrograph specimens were fine polished then etched with Keller's reagent.

Defects obtained from the welds made include trenching (TR), wormhole (WH), incomplete penetration (IP), underfill/flash (UF/F), and internal void (IV) defects. The weld quality classes were divided into three categories: hot, nominal, and cold. This categorization is based upon the impact that the process

Table 1 Data-driven modeling works that pertain to FSW aiming to predict weld quality

Ref.	Objective	Technique	Input type	Feature extraction
[22]	Prediction of UTS	ANFIS and ANN	PP	None
[23]	Development of wormhole detection method	ANN	SF	DFT
[24]	Prediction of UTS and YS	ANN	SF	WPT
[25]	Utilize MP, weld quality, and average grain size for training and prediction of fuzzy models	FHMO-FM	MP, PP	None
[26]	Development of surface quality monitoring technique	SVM	SF	DWT
[27]	Prediction of internal defect formation	SVM, ANN	SF, PP	DWT
[28]	Prediction of hardness and UTS	ANN	PP	None
[29]	Prediction of surface weld quality	ANN	SF	FFT
[30]	Prediction of mechanical properties	DT	PP	None
[31]	Prediction of UTS	Regression	SF	Frac. T
[32]	Prediction of UTS	None	SF	Frac. T, DWT
[33]	Development of defect formation monitoring scheme	None	SF	DWT
[34]	Development of defect formation monitoring scheme	None	SF	Fract. T
[35]	Development of acoustic emission defect formation monitoring scheme	None	SF	FFT, STFT, DWT

ANFIS adaptive neuro-fuzzy inference system, *ANN* artificial neural network, *DFT* discrete Fourier transform, *Frac.*, T-fractal theory, *DT* decision tree, *DWT* discrete wavelet transform, *FFT* fast Fourier transform, *STFT* short-time Fourier transform, *FHMO-FM* fast hierarchical multi-objective fuzzy modeling, *SVM* support vector machine, *UTS* ultimate tensile strength, *WPT* wavelet packet transformation, *YS* yield strength

parameters have on the joint quality and observable defects. Hot welds have relative characteristics of excessive heat input introduced by high spindle rotational speed, low feed rate, and high plunge force. Hot welds exhibited UF/F defects where metal was expelled from the weld seam. Internal voids were also found in this category located in the stir zone on the advancing side (AS) of the weld. Alternatively, cold welds are attributed to low heat input caused by low spindle rotational speed, high feed rate, and low plunge force. A cold weld schedule produces the WH, IP, and TR defect types. Lastly, nominal welds refer to welds with no detectable defects. Figure 2 illustrates as-welded panel surfaces and transverse sectional macrographs of selected specimens from each category.

Once each weld was evaluated and classified, trends in the data that could be related to individual process parameters were observed. In order to create a link between these parameters, a pin speed ratio (PSR) and a parameter-coined empirical force index (EFI) that encompasses all three process parameters with pin tool geometric conditions were devised [22]. These two relations can be observed in Eqs. 1 and 2.

$$PSR = 2\pi r \cdot \frac{\omega}{V} \tag{1}$$

$$EFI = \frac{F_z}{C_1 (PSR)^{-C_2}} \tag{2}$$

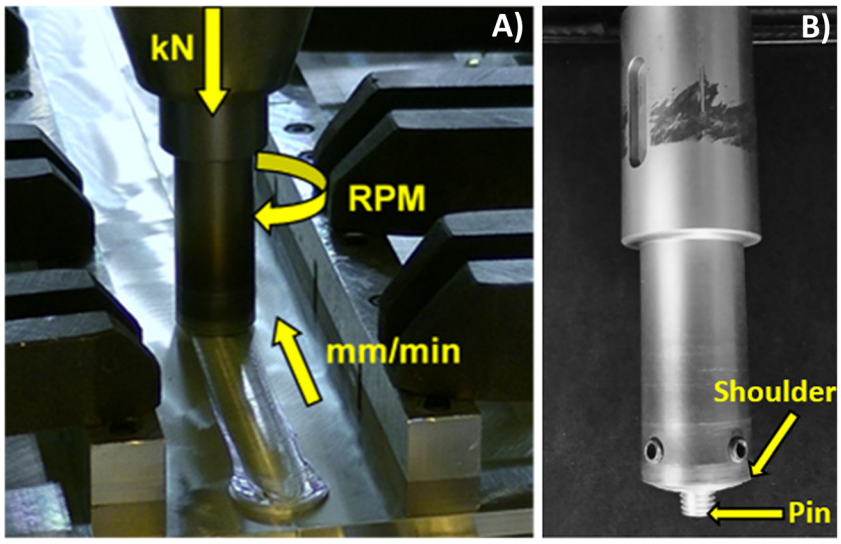

Fig. 1 **a** FSW configuration employed in this work during operation illustrating the three process parameters that compose a weld schedule. **b** An image of the fixed pin tool illustrating pin and shoulder

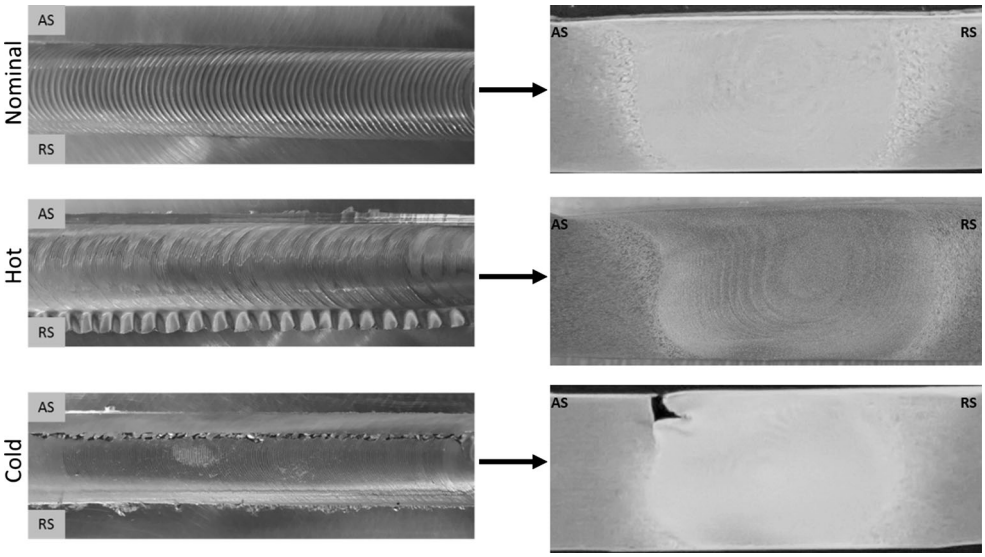

Fig. 2 Plan surfaces (left) and transverse sections (right) of a nominal, hot, and cold weld specimen

where V denotes feed rate, ω is spindle rotational speed, r is the pin radius, F_z is plunge force, and C_1 and C_2 are constants obtained from the curve of nominal experimental data points from the process parameter plot in Fig. 3. The classification of welds in this study can be roughly indicated by the EFI. The EFI relation determines if the process parameters are near nominal welding conditions. If the value is near 1, nominal welding conditions should occur. If the EFI value deviates from unity, then the weld quality deteriorates. The EFI is meant to be utilized to estimate weld quality with few data points to help guide the prediction of nominal welding conditions. In [22], the EFI was employed to obtain defect-free joints. This relation is valuable for modeling as it relates the three process parameters for FSW. The numerical ranges for each quality classification can be observed in Table 2. The constants C_1 and C_2 in this study were found to be 245.43 and 0.551, respectively.

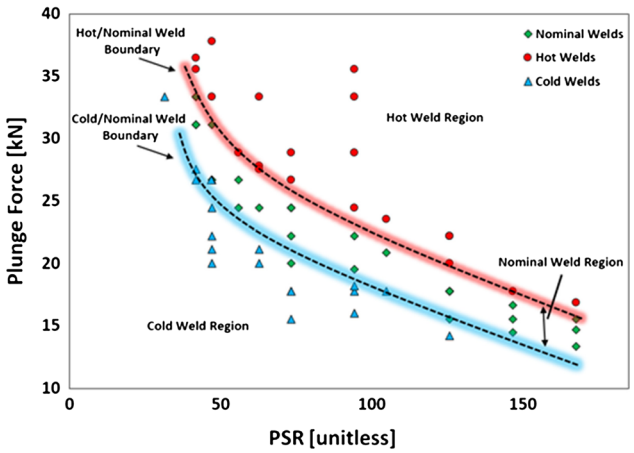

Fig. 3 Process parameter window illustrating weld quality classes and the boundaries between hot and nominal as well as cold and nominal weld conditions

It is observed there is overlap in EFI values for regions approaching 1.00. In this region, overlapping EFI values are due to the boundary that dictates a hot/nominal and cold/nominal weld condition. From the ranges above, the overlap of maximum and minimum EFI values for cold-nominal conditions has a range of 0.09 and for nominal-hot 0.03. The determination of quality in these regions is dictated by mechanical properties and observed defects. At these regions, there is a propensity for process parameters to create either nominal or inferior properties. In order to zero-in on these boundaries, many more experiments must be conducted and were not able to be further investigated in this study due to budget constraints. The EFI ranges with respect to mechanical properties can be visualized in Fig. 4.

2.3 FSW signal features

During the welding process, FSW signals were recorded at a sampling rate of 60 Hz by the welding machines that include X-force, Y-force, plunge force, RPM, and feed rate. Typically, in manufacturing settings, signal data is only viewed with a low sampling rate, i.e., 10 Hz. However, it was conjectured that this signal data sampled at higher rates might lead to indication of defects or instability in a weld due to the information that can be obtained from the variation in signal data. As an example, Fig. 5 illustrates a weld where a defect has occurred. In this weld, the initial plunge stage creates a defect-free welding environment as adequate pre-heating of material near the pin tool occurs in the plunge and dwell stage. As the pin tool traverses the seam, the heat generated from those stages dissipates leading to a defective weld roughly 150 mm into the weld. The force signals have a sudden change in magnitude at the point where a defect-free region turns into a defect region, as highlighted by the circle in Fig. 5.

Table 2 Weld quality values for EFI with associated averages

	EFI range	Average
Cold	0.68–0.96	0.83
Nominal	0.87–1.11	1.00
Hot	1.08–1.77	1.26

The signals acquired for each weld experiment generated large data sets which poses problems for classification algorithms. Moreover, signal data obtained during FSW is highly uniform due to the load-control process employed in this study; consequently, a large portion of the signal data collected is somewhat redundant. Extraction of useful features requires a signal processing technique that will map the existence of frequency components in the signal and produce a representation of how these components change during welding. The discrete wavelet decomposition (DWD) method provides a signal processing technique that meets all the criteria for extracting useful features from FSW signals. These features can identify frequencies and their magnitudes at specific points in time and can be represented in multiple resolutions. For this reason, the DWD method was employed to analyze the weld signals acquired during FSW experiments.

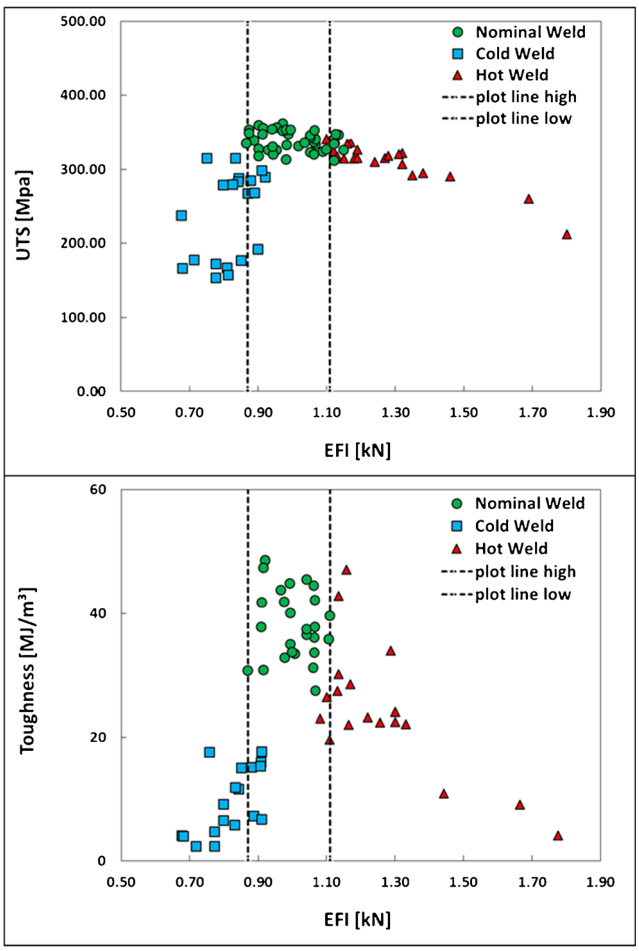

Fig. 4 Weld quality classes based upon EFI, UTS, and toughness

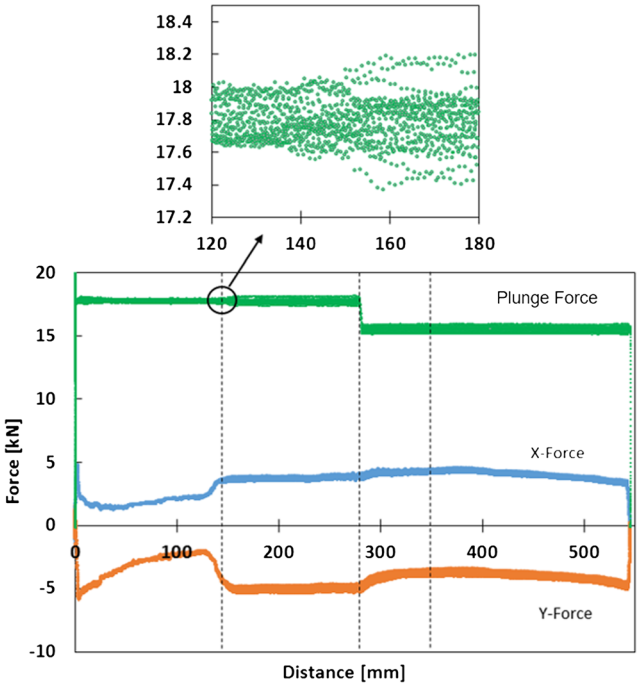

Fig. 5 FSW signal data illustrating weld signal data of X-force, Y-force, and plunge force indicating the change in steady-state conditions when a TR defect forms

Before the application of DWD, the original FSW signals were segmented into discrete segments. Segmentation is conducted in a way to ensure no overlapping of windows occurs and the data size in each window will change for varying feed rates. Wavelet methods were thereafter applied separately to each window. In this work, the first order Daubechies (Haar) wavelet was chosen as the mother wavelet due to its computational efficiency. The basis of DWD is the filtering schemes which provide the capability to decompose the original signal into different details as seen in Eqs. (3) and (4).

$$y_{HighPassFilter}(k) = \sum_{n} x(n)\cdot g(2k-n) \tag{3}$$

$$y_{LowPassFilter}(k) = \sum_{n} x(n)\cdot h(2k-n) \tag{4}$$

Upon the completion of the wavelet calculation for one window, the output was saved and the process was repeated for adjacent windows until all windows undergo wavelet transformation. This process was repeated for up to five levels of decomposition to construct five sets of details for each signal type. The energy of each decomposed set of details is computed as the sum of the squares of its values. Hence, for each segment of weld, five energy values are extracted from each signal. Exact details of this feature extraction process can be found in [40], and part of the resultant features employed in this study are given in Appendix 2.

3 Classification methodology

Two classification algorithms, specifically KNN and FKNN, were employed to build classification models utilizing only process-related parameters first, and then with additional signal features later for potential classification accuracy improvement. In this work, the number of folds for cross-validation is varied from twofold, tenfold, to LOOCV to determine best classification result. The reason for employing these three was decided to double check whether different folds would lead to different results. These techniques are popular in the literature and are utilized to evaluate the performance of classification algorithms; however, attention to the approaches for making statistical inferences must be considered when using the said techniques [49] such as the number of folds, number of instances in a fold, the averaging for accuracy estimation, and the repetition of K-fold cross-validation. KNN and FKNN are known as lazy learning methods with only one model parameter, i.e., K. These techniques were selected for this study due to their ease of use, and no need for training the model in serving as the classifier in the wrapper approach of metaheuristic-based feature selection.

Metaheuristics, which are high-level strategies for exploring search spaces, are a proven technique to determine the optimal feature subsets and can be exercised to optimize a classification modeling scheme. Feature selection is a promising technique for building a better classification model with fewer more discriminant features, and such an approach has been successfully applied to weld applications to produce good results [13, 41, 42]. In order to improve classification accuracy, a proven metaheuristic algorithm ABC [43] is chosen for this study to be employed for not only feature selection but also optimizing model parameter K of KNN and FKNN. It is noted that ABC has been employed for feature selection in past works [43–47], but none on weld quality prediction. Two of these three papers employed KNN as the classifier, but the *K* value in these works was not optimized but assumed to be one. In [44], ABC was utilized to select features to classify UCI repository data sets such as image segmentation, automotive, and health issues. In that study, results indicate that a reduced number of features can achieve improved classification accuracy compared to using every feature. ABC outperformed other algorithms in eight out of ten tested data sets. Another study employed ABC for feature selection and utilized SVM to classify images in medical applications [45]. In that study, it was determined that the said method is more successful compared to other pattern recognition algorithms. Reference [48] utilized ABC to perform feature selection on bioinformatics. In that study, KNN was employed for fitness evaluation and found high classification accuracy for large and small data sets. Another study employed ABC coupled with neural network as the classifier to select optimal feature subsets [47]. The feature selection technique was tested on six data sets from UCI machine learning repository. Comparing ABC with other optimization techniques coupled with neural network, it was found that ABC obtained best performance.

It is evident ABC is a suitable technique for feature selection and is quite useful when coupled with a classification method. Furthermore, ABC is widely accepted due to its straightforward implementation and it has few control parameters. The ABC algorithm imitates honey bee's behavior in selecting food sources. To accomplish this, bees are divided into three groups that include the employed, onlooker, and scout bees. The food source in ABC represents a solution in optimization problems, which is a feature subset in the context of this study. An outline of the algorithm and functions of the bee groups are presented below:

Start:

Initialize solutions
Repeat

1) Employed bee process

Update and evaluate feasible solutions

2) Onlooker bee process

Select feasible solutions
Update and evaluate feasible solutions

3) Scout bee process

Avoid sub-optimal solutions (replace them with randomly generated solutions)

Continue until maximum number of iterations/stopping criterion met.

End

The number of employed bees is equal to the number of food sources, i.e., solutions to an optimization problem. The employed bees determine the probability value of sources and share the information with the onlooker bees. The probability of a food source (or feature subset solution) *i* is computed as:

$$p_i = 0.9^{*}\frac{fitness_i}{\max\limits_{\forall i}(fitness_i)} + 0.1 \tag{5}$$

$$fitness_i = \frac{1}{\mathrm{err}_i + 1} \tag{6}$$

where err_i denotes the error rate for a feature subset solution *i*, computed as the number of misclassified data points over number of tested data points.

Thereafter, the onlooker bees use said information to determine whether a particular food source should be pursued.

Table 3 Classification error rates for weld quality utilizing KNN and FKNN with all features

	K-fold = 2 Classification error (%)	K-fold = 10 Classification error (%)	LOOCV Classification error (%)
KNN	35.53	28.57	25.40
FKNN	40.79	32.86	33.33

Both employed and onlooker bees use the following equation to generate a new solution v_i from x_i [49].

$$v_{ij} = x_{ij} + \varnothing_{ij}\left(x_{ij} - x_{kj}\right) \tag{7}$$

where k is a randomly selected solution different from i (or food source visited by a bee), j is a randomly selected dimension, and ϕ_{ij} is a random number $\in[-1, 1]$. The scout bees are responsible for searching for new food sources, and the new solution is often randomly generated.

The ABC algorithm was originally developed for continuous optimization. To use it for feature selection, real values between zero and one are rounded into binary with 1(0) indicating a feature selected (not selected). The K values range from 1 to half of the total number of data records, and a rounding operation has to be applied to convert a real-coded K into an integer K as well.

4 Results and discussion

4.1 Stand-alone classifier model versus metaheuristic with classifier wrapper

At the on-set of the work, KNN and FKNN were tested to determine which classification algorithm would produce the best result using the data listed in Appendix 1. In other words, all process parameter-related features are employed without feature selection. The K value is assumed to be 1 for both KNN and FKNN. It was observed that KNN outperformed FKNN in all cases regardless of the cross-validation scheme. The general trend of increasing classification accuracy is expected as the number of folds increases, as shown in Table 3. The classification error is the ratio of number of errors and number of data points tested over all K-fold tests. The predictability of the model is of interest here; hence, the model training error was not computed.

In order to improve classification accuracy, ABC was employed for selecting near-optimal feature subset and obtaining a near-optimal K value. Table 4 illustrates the results by varying the three CV schemes and population size. Simulations were extended until convergence was achieved as seen in Fig. 6. The maximal number of evaluations was set at 10,000, which is a bit too large because the convergence seems to occur early. To capture the stochastic nature of ABC, ten runs were made. Comparing Table 4 with Table 3, it is observed that model classification error rates are lower when KNN and FKNN are used together with ABC-based feature selection, regardless the CV scheme. When the ABC metaheuristic is applied to determine the features to be utilized and the optimal K value in the classification algorithm, classification error reduces.

The results in Table 4 illustrate the average classification error and standard deviation for ten runs of the ABC algorithm. In the majority of cases with KNN, the optimal K value obtained was 1. In few cases, namely when the K-fold = 2 technique was employed, the optimal K value varied from 6 to 9. Furthermore, the best feature subset obtained from each case also varied when K-fold = 2 but were all similar when K-fold = 10 and when LOOCV was employed. This trend remained the same as the population size increased. On the other hand, for FKNN, the optimal K value varied from 6 to 7 when K-fold = 2. In every other CV technique, the optimal K

Table 4 Classification error rates of weld quality for KNN and FKNN coupled with metaheuristic ABC

	K-fold = 2		K-fold = 10		LOOCV	
	Avg. classification error (%)	St. Dev.	Avg. classification error (%)	St. Dev.	Avg. classification error (%)	St. Dev.
Population size = 5						
KNN +ABC	19.16	0.01	11.73	0.03	8.40	0.04
FKNN + ABC	24.21	0.01	13.69	0.02	11.54	0.03
Population size = 10						
KNN + ABC	18.74	0.01	10.54	0.02	6.84	0.01
FKNN + ABC	23.81	0.01	13.19	0.01	9.97	0.01
Population size = 15						
KNN + ABC	18.79	0.01	11.01	0.03	7.19	0.02
FKNN + ABC	23.92	0.04	14.04	0.02	10.97	0.03

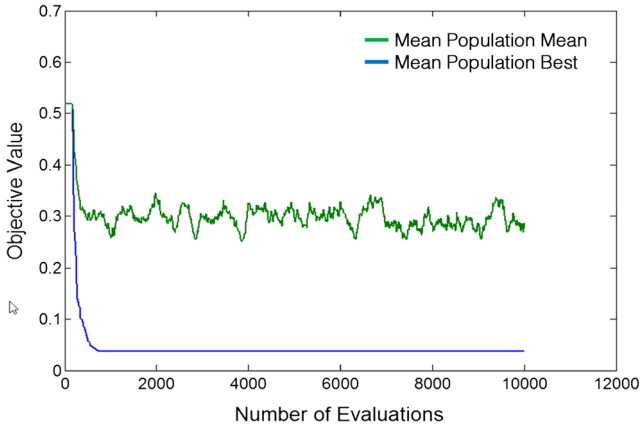

Fig. 6 Convergence profile of KNN + ABC where population size = 10 with tenfold CV

value obtained varied from 1 to 2. The best feature subsets for each case regardless of the CV technique and population size remained the same.

The results indicate that the best model achieved the average classification error of 6.84% based on LOOCV when KNN is coupled with ABC using a population size of 10. The best feature subset included rotational speed, feed rate, and EFI with optimal *K* value of 1. KNN again outperforms FKNN and accuracy again increases with number of folds. The low standard deviation values indicate the consistency of the ABC algorithm in producing similar results. Comparing the results of three population sizes, the population size of 10 appears to be the best.

The weld schedules (or process parameters) which promote the decrease in weld classification accuracy are identified in Table 5. These have been identified as weld schedules which are on the boundaries between hot/nominal and cold/nominal welds as discussed in the above section. At this region, the quality of a weld schedule is hard to predict as the process parameter combination may or may not lead to a nominal weld, as seen in the process parameter window in Fig. 3. In the nominal weld region, the combination of weld parameters provides sufficient heat and mechanical deformation to join the faying surfaces of the two workpieces. If any one of these parameters are varied, the material flow characteristics will change and cause adverse properties. For certain weld parameter combinations, there is a region where the combination begins to degrade the joint quality. As an example, if rotational speed and feed rate are taken to be constant and the plunge force is varied, a clear difference in weld quality will be obtained going from low to high. Alternatively, taking the plunge force to be constant and varying the combination of rotational speed and feed rate, the weld quality will also be altered. These combinations of weld parameters are more sensitive at the hot/nominal and cold/nominal boundaries. This is why in industry and production settings, considerable time and effort are employed to choose the best weld schedule for an application, and one that is conservative in that the process parameter combination, if altered due to an anomaly, will retain satisfactory joint quality.

Table 5 Weld schedules which promote inacurrate classification due to having a combination of process parameters which lie on the boundaries of hot/nominal and cold/nominal weld quality (3—hot weld, 8—cold weld)

RPM	Feed rate (mm/min)	Plunge force (kN)	Quality class
300.00	152.40	27.80	3
300.00	152.40	27.58	3
400.00	228.60	28.91	3
450.00	76.20	14.46	2
200.00	152.40	27.58	2
300.00	101.60	17.79	2
200.00	135.38	26.69	2
200.00	203.20	33.36	2
250.00	170.18	26.69	2
450.00	152.40	18.24	2
250.00	76.20	17.79	2

To illuminate the inaccuracy of the boundary regions (points located at the boundary are prone to classification error), the aforementioned modeling and testing schemes were repeated without the boundary data sets that breach into the nominal weld region. Thus, any data points classified with an EFI outside the range of 0.68–0.87 for cold welds and 1.11–1.77 for hot welds were temporarily removed (eight cold welds and three hot welds) for demonstration purposes (they are put back in the subsequent tests). The results of this test can be observed in Tables 6 and 7. Comparing Table 6 with Table 3, and Table 7 with Table 4, it can be found that classification accuracy increases for all cases when boundary data points are removed. KNN again outperforms FKNN and accuracy again increases with number of folds. The low standard deviation values again indicate the consistency of the ABC algorithm in producing similar results. Comparing the results of three population sizes, population size of 15 appears to be the best but is only slightly better than 10.

The best feature subset produced which obtained the best classification accuracy was EFI alone with a *K* value of 2. This

Table 6 Classification error rates for weld quality utilizing KNN and FKNN with all features without boundary data sets

	K-fold = 2 Classification error (%)	K-fold = 10 Classification error (%)	LOOCV Classification error (%)
KNN	25.93	21.30	22.92
FKNN	34.03	25.00	24.20

Table 7 Classification error rates of weld quality for KNN and FKNN coupled with metaheuristic ABC without boundary data sets

	K-fold = 2		K-fold = 10		LOOCV	
	Avg. classification error (%)	St. Dev.	Avg. classification error (%)	St. Dev.	Avg. classification error (%)	St. Dev.
Population size = 5						
KNN +ABC	3.70	0.00	2.50	0.00	2.70	0.01
FKNN +ABC	16.67	0.00	15.50	0.02	16.02	0.01
Population size = 10						
KNN + ABC	3.70	0.00	2.5	0.00	2.26	0.00
FKNN + ABC	16.67	0.00	14.70	0.03	15.26	0.01
Population size = 15						
KNN + ABC	3.70	0.00	2.39	0.00	2.18	0.00
FKNN + ABC	16.67	0.00	14.01	0.02	15.44	0.01

result is intuitive as EFI incorporates all three process parameters and now better defines the quality due to omitting the boundary region overlap data. This illuminates the difficulties employing only input features of rotational speed, feed rate, plunge force, and relations which incorporate those three parameters. Ideally, if the boundary regions are definitive, then high accuracy rates can be achieved as seen here. However, in reality, this is not the case because the boundary regions near defect and defect-free welding conditions are blurry. To circumvent the issue of the boundary region classification, weld signal features were subsequently added to the input data pool to determine if an improved classification model could be constructed.

4.2 Weld signal features added to classification models

Weld signals are important to understand the quality of a weld. During the weld process, it is a standard practice for the operator to monitor weld signals to ensure forces acting on the pin tool do not exceed a predetermined value based upon weld tooling. Furthermore, viewing the fluctuations in signal values can indicate quality of the weld as observed by previous research summarized in Table 1. The operator has the discretion to abort a weld if a target value or large fluctuation in a particular weld signal is observed. This study attempts to show that automatic interpretation of weld signals can greatly assist the operator in predicting the quality of a weld.

Our study aims to use signal features to strengthen the correlation between the three process parameters and weld quality. As discussed in Section 2, DWD was employed to obtain these features. In total, five signal types including X-force, Y-force, plunge force, rotational speed, and feed rate signals were fed into the DWD algorithm window by window to extract features. For each signal type, five decomposition levels were obtained. The window size for DWD was computed as a function of weld travel distance rather than time. Features from three of these windows were chosen based upon three locations at the start, middle, and end of the weld to ensure features at all locations of the weld are caught.

In order to determine the weld signal features which promote the best classification result, the set of five features from each signal was added to the set of process parameters and tested with KNN and FKNN classifiers. To avoid redundancy, the tests conducted here utilized only LOOCV. The population size of the ABC algorithm was increased to 20 as a larger data set was fed into the model classification scheme.

A summary of results from ten runs are given in Table 8 with best feature subset and optimal K value. In all cases with KNN, the optimal K value obtained was 1; however, the best feature subset varied from run to run. The best features reported in Table 8 are the most common obtained from the ten runs. For KNN, the best feature subset was obtained five times for plunge force wavelet features (WFs), six times for X-force WFs, four times for Y-force WFs, four times for RPM WFs, and four times for feed rate WFs. On the other hand, for FKNN, the optimal K value deviated from 1 for cases that employed RPM and X-force WFs. However, the most common K value obtained in those cases was 1. The best features listed in Table 8 for FKNN were obtained five times for plunge force WFs, four times for X-force WFs, three times for Y-force WFs, four times for RPM WFs, and six times for feed rate WFs.

It was found that adding weld signal features significantly improved the classification accuracy. In seven of the ten cases, 100% accuracy was obtained. In the three cases which did not obtain 100% accuracy, the FKNN technique was utilized as the classifier. Overall, incorporating weld signal features to the model improved the accuracy and mitigates the issues that the boundary region creates for the model. Comparing the result of each set of wavelet signal features, it appears that each

Table 8 Classification error rates of weld quality for KNN and FKNN coupled with metaheuristic ABC employing additional features obtained from weld signals

Features added		Best feature subset (found by the ABC algorithm)											Classification error	
		K number	RPM	FR (mm/min)	PF (kN)	PSR	EFI (kN)	WF 1	WF 2	WF 3	WF 4	WF 5	Mean (%)	St. Dev.
Plunge force wavelet features	KNN	1	√		√		√		√	√		√	0.0	0.0
	Fuzzy KNN	1	√	√			√	√	√	√	√	√	22.50	0.0
X-force wavelet features	KNN	1			√	√		√					0.0	0.0
	Fuzzy KNN		√	√			√	√	√	√			0.60	0.0
Y-force wavelet features	KNN	1		√	√		√	√	√				0.0	0.0
	Fuzzy KNN	1				√	√	√	√				0.0	0.0
RPM wavelet features	KNN	1	√	√		√	√			√			0.0	0.0
	Fuzzy KNN	1	√	√	√		√			√			0.0	0.0
Feed rate wavelet features	KNN	1	√	√	√	√	√	√		√			0.0	0.0
	Fuzzy KNN	1	√				√	√	√	√		√	12.33	0.01

provides the best result when KNN is applied. However, if FKNN is taken as the classification technique, then plunge force, X-Force, and feed rate signal features should not be utilized. For this reason when developing a classification algorithm for FSW, utilization of weld signal features should be conducted to produce the best model for predicting weld quality more accurately.

Among the seven cases that yield perfect classification accuracy, the best case can be chosen to be the one with lowest number of features. Consequently, the best feature subset comprised of plunge force, pin speed ratio, and the first wavelet feature of the X-force signal (the third row in Table 8) should be used to build the 1-NN model. The next best model is the fuzzy 1-NN model built with four features, which are PSR, EFI, and the first and second wavelet features of the Y-force signal (the sixth row in Table 8).

5 Conclusions

This paper has presented the results obtained in a study to build a reliable and highly accurate weld quality prediction model. From an extensive experimental FSW study, KNN- and FKNN-based classification models for weld quality prediction were built employing weld process parameters, a pin speed ratio, an empirical relation, and wavelet features extracted from weld signal data. Employing only the welding process parameters as inputs, moderate classification accuracy was obtained due to the fuzzy boundaries of hot/nominal and cold/nominal welds. The test results indicate that employing the population-based metaheuristic artificial bee colony, classification accuracy improves as opposed to using all features to build classification models. One hundred percent classification accuracy was obtained utilizing ABC with KNN or ABC with FKNN while incorporating weld signal features. In order to build the best model with highest classification accuracy, weld signal features should be employed together with process parameters.

A high number of classification models and metaheuristic algorithms have been developed. If used properly, it is expected that any combination will achieve similar results as reported in this study, though they might differ in the best result. Since 100% accuracy has been achieved in the study, no attempt in using other combinations of classification model and metaheuristic is necessary. However, the combination used in this study might not be the best for another application.

Acknowledgments The authors would like to gratefully acknowledge the support received from the National Aeronautics and Space Administration (NASA) via NASA-SLS grant no. NNM13AA02G

Appendix 1. Friction stir weld quality data without signal features

Table 9 Quality classification with associated weld schedule, pin speed ratio, and EFI

Number	RPM	Feed rate (mm/min)	Plunge force (kN)	Pin speed ratio	EFI (kN)	Quality
1	300.00	152.40	21.13	62.83	0.84	2
2	300.00	152.40	24.47	62.83	0.98	1
3	350.00	152.40	17.79	73.30	0.77	2
4	350.00	152.40	15.57	73.30	0.68	2
5	200.00	152.40	26.69	41.89	0.85	2
6	200.00	152.40	33.36	41.89	1.06	1
7	450.00	152.40	33.36	94.25	1.66	3
8	450.00	152.40	28.91	94.25	1.44	3
9	450.00	152.40	35.59	94.25	1.77	3
10	300.00	203.20	21.13	47.12	0.72	2
11	300.00	203.20	24.47	47.12	0.83	2
12	350.00	76.20	15.57	146.61	0.99	1
13	300.00	152.40	20.02	62.83	0.80	2
14	300.00	203.20	22.24	47.12	0.76	2
15	300.00	203.20	20.02	47.12	0.68	2
16	350.00	118.62	19.57	94.18	0.99	1
17	350.00	152.40	17.79	73.30	0.77	2
18	450.00	76.20	14.46	188.50	0.96	2
19	200.00	152.40	31.14	41.89	0.91	1
20	300.00	203.20	26.69	47.12	0.91	1
21	200.00	152.40	27.58	41.89	0.88	2
22	225.00	152.40	37.81	47.12	1.29	3
23	300.00	152.40	33.36	62.83	1.33	3
24	350.00	152.40	28.91	73.30	1.26	3
25	300.00	101.60	16.01	94.25	0.80	2
26	300.00	101.60	24.47	94.25	1.22	3
27	350.00	88.90	15.57	125.66	0.92	1
28	350.00	88.90	22.24	125.66	1.30	3
29	300.00	152.40	27.80	62.83	1.11	3
30	350.00	76.20	14.46	146.61	1.06	1
31	350.00	76.20	16.68	146.61	1.06	1
32	300.00	76.20	14.23	125.66	0.83	2
33	300.00	152.40	27.58	62.83	1.10	3
34	350.00	76.20	17.79	146.61	1.13	3
35	300.00	130.56	24.47	73.34	1.11	1
36	350.00	152.40	26.69	73.30	1.16	3
37	350.00	88.90	20.02	125.66	1.17	3
38	300.00	101.60	22.24	94.25	1.04	1
39	300.00	101.60	17.79	94.25	0.89	2
40	200.00	135.38	26.69	47.15	0.91	2
41	300.00	76.20	17.79	125.66	1.04	3
42	400.00	101.60	17.79	125.66	1.07	3
43	400.00	76.20	15.57	167.55	1.04	3
44	200.00	203.20	33.36	31.42	0.91	2
45	350.00	88.90	17.79	125.66	0.97	1
46	350.00	152.40	22.24	73.30	0.87	1
47	350.00	152.40	20.02	73.30	1.06	1

Table 9 (continued)

Number	RPM	Feed rate (mm/min)	Plunge force (kN)	Pin speed ratio	EFI (kN)	Quality
48	250.00	170.18	26.69	46.89	0.91	2
49	450.00	152.40	18.24	94.25	0.91	2
50	200.00	152.40	36.48	41.89	1.16	3
51	350.00	152.40	24.47	73.30	1.01	1
52	400.00	76.20	16.90	167.55	1.16	3
53	400.00	76.20	14.68	167.55	0.91	1
54	300.00	76.20	22.24	125.66	1.30	3
55	400.00	76.20	13.34	167.55	1.11	1
56	250.00	76.20	23.58	104.72	1.25	3
57	250.00	76.20	17.79	104.72	0.94	2
58	250.00	76.20	20.91	104.72	1.06	1
59	300.00	203.20	31.14	47.12	1.06	1
60	300.00	203.20	33.36	47.12	1.14	3
61	300.00	228.60	33.36	41.89	0.99	1
62	300.00	228.60	35.59	41.89	1.14	3
63	300.00	228.60	31.14	41.89	0.91	1
64	400.00	228.60	28.91	55.85	1.08	3
65	400.00	228.60	24.47	55.85	1.00	1
66	400.00	228.60	26.69	55.85	0.99	1

Appendix 2. Selected data is presented here; the entire data set will be made available to public if funding agency agrees to release

Table 10 Quality classification with associated weld schedule, pin speed ratio, EFI, and X-force wavelet features

						Wavelet features of X-force, window 1					
Number	RPM	Feed rate (mm/min)	Plunge force (kN)	Pin speed ratio	EFI (kN)	WF 1	WF 2	WF 3	WF 4	WF 5	Quality
1	300.00	152.40	21.13	62.83	0.87	0.0013	0.0038	0.0005	0.0001	0	2
2	300.00	152.40	24.47	62.83	1.01	0.0016	0.0006	0.0071	0.002	0.0009	1
3	350.00	152.40	17.79	73.30	0.80	0.0365	0.0063	0	0.0076	0.0038	2
4	350.00	152.40	15.57	73.30	0.70	0.023	0.0078	0.0092	0.0002	0.0101	2
5	200.00	152.40	26.69	41.89	0.88	0.074	0.0279	0.0033	0.0001	0.0016	2
6	200.00	152.40	33.36	41.89	1.10	0.5096	1.6194	4.1275	5.7191	24.3126	1
7	450.00	152.40	33.36	94.25	1.71	0.0657	0.261	0.6624	0.0495	0.0003	3
8	450.00	152.40	28.91	94.25	1.49	0.164	0.221	1.9316	0.0307	0.119	3
9	450.00	152.40	35.59	94.25	1.83	0.0344	0.1343	0.3605	0.735	0.011	3
10	300.00	203.20	21.13	47.12	0.74	0.1657	0.4024	1.2995	0.3135	0.0492	2

Table 11 Quality classification with associated weld schedule, pin speed ratio, EFI, and Y-force wavelet features

						Wavelet features of Y-force, window 1					
Number	RPM	Feed rate (mm/min)	Plunge force (kN)	Pin speed ratio	EFI (kN)	WF 1	WF 2	WF 3	WF 4	WF 5	Quality
1	300.00	152.40	21.13	62.83	0.87	0.0094	0.0014	0.0274	0.0077	0.0009	2
2	300.00	152.40	24.47	62.83	1.01	0.0061	0.016	0.0043	0.0007	0.0003	1
3	350.00	152.40	17.79	73.30	0.80	0.0693	0.0491	0.0002	0.0261	0.0145	2
4	350.00	152.40	15.57	73.30	0.70	0.0417	0.0298	0.0029	0	0.0034	2
5	200.00	152.40	26.69	41.89	0.88	0.0752	0.0003	0.0015	0.0001	0.0021	2
6	200.00	152.40	33.36	41.89	1.10	0.1512	0.5686	1.3644	2.4082	6.3846	1
7	450.00	152.40	33.36	94.25	1.71	0.0535	0.1483	0.2872	0.0002	0.0254	3
8	450.00	152.40	28.91	94.25	1.49	0.257	1.2951	0.0684	0.0046	0.0179	3
9	450.00	152.40	35.59	94.25	1.83	0.2579	1.0236	3.2396	3.8241	0.1033	3
10	300.00	203.20	21.13	47.12	0.74	0.1413	0.4645	0.9784	0.2266	0.2907	2

Table 12 Quality classification with associated weld schedule, pin speed ratio, EFI, and plunge force wavelet features

						Wavelet features of plunge force, window 1					
Number	RPM	Feed rate (mm/min)	Plunge force (kN)	Pin speed ratio	EFI (kN)	WF 1	WF 2	WF 3	WF 4	WF 5	Quality
1	300.00	152.40	21.13	62.83	0.87	0.0005	0.0001	0.0032	0.0007	0.0002	2
2	300.00	152.40	24.47	62.83	1.01	0.0003	0.0016	0.001	0.0003	0.0004	1
3	350.00	152.40	17.79	73.30	0.80	0.0012	0.0008	0	0.0001	0.0001	2
4	350.00	152.40	15.57	73.30	0.70	0.0024	0.0026	0.0012	0	0.0015	2
5	200.00	152.40	26.69	41.89	0.88	0.0128	0	0.0008	0	0.0009	2
6	200.00	152.40	33.36	41.89	1.10	0.0002	0.0003	0.0004	0	0	1
7	450.00	152.40	33.36	94.25	1.71	0.0003	0.0005	0.001	0.0001	0	3
8	450.00	152.40	28.91	94.25	1.49	0.0003	0.0008	0.0013	0	0	3
9	450.00	152.40	35.59	94.25	1.83	0	0	0.0001	0.0001	0	3
10	300.00	203.20	21.13	47.12	0.74	0.0002	0.0002	0.0004	0.0001	0	2

Table 13 Quality classification with associated weld schedule, pin speed ratio, EFI, and rotational speed wavelet features

						Wavelet features of rotational speed, window 1					
Number	RPM	Feed rate (mm/min)	Plunge force (kN)	Pin speed ratio	EFI (kN)	WF 1	WF 2	WF 3	WF 4	WF 5	Quality
1	300.00	152.40	21.13	62.83	0.87	0.0026	0.0027	0.0085	0.003	0	2
2	300.00	152.40	24.47	62.83	1.01	0.025	0.0823	0.198	0.047	0.0433	1
3	350.00	152.40	17.79	73.30	0.80	0.1631	0.1112	0.0009	0.0081	0.0013	2
4	350.00	152.40	15.57	73.30	0.70	0.0583	0.0408	0.0003	0	0.0007	2
5	200.00	152.40	26.69	41.89	0.88	0.179	0.1069	0.0635	0	0.0609	2
6	200.00	152.40	33.36	41.89	1.10	2.5883	7.2243	13.5473	1.2495	1.6578	1
7	450.00	152.40	33.36	94.25	1.71	0.5032	1.32	3.1739	0.2163	0.0004	3
8	450.00	152.40	28.91	94.25	1.49	5.1294	1.73	23.8277	0.047	0.0368	3
9	450.00	152.40	35.59	94.25	1.83	0.2578	0.9887	2.5092	3.906	0.004	3
10	300.00	203.20	21.13	47.12	0.74	0.4339	1.1813	4.0631	0.8472	0.4385	2

Table 14 Quality classification with associated weld schedule, pin speed ratio, EFI, and feed rate wavelet features

						Wavelet features of feed rate, window 1					
Number	RPM	Feed rate (mm/min)	Plunge force (kN)	Pin speed ratio	EFI (kN)	WF 1	WF 2	WF 3	WF 4	WF 5	Quality
1	300.00	152.40	21.13	62.83	0.87	0.0028	0.0026	0.0036	0.0013	0.0004	2
2	300.00	152.40	24.47	62.83	1.01	0.0059	0.0089	0.004	0.0005	0.0003	1
3	350.00	152.40	17.79	73.30	0.80	0.0085	0.0015	0.0002	0.0035	0.0029	2
4	350.00	152.40	15.57	73.30	0.70	0.0104	0.0071	0.0069	0.0004	0.0023	2
5	200.00	152.40	26.69	41.89	0.88	0.0053	0.0019	0.0003	0	0.0001	2
6	200.00	152.40	33.36	41.89	1.10	0.0001	0.0001	0.0001	0	0	1
7	450.00	152.40	33.36	94.25	1.71	0.0001	0.0004	0.0009	0	0	3
8	450.00	152.40	28.91	94.25	1.49	0.0001	0.0001	0.0001	0	0	3
9	450.00	152.40	35.59	94.25	1.83	0.0007	0.002	0.0052	0.0077	0.0001	3
10	300.00	203.20	21.13	47.12	0.74	0.0006	0.002	0.0046	0.0011	0.0003	2

References

1. Çam G, İpekoğlu G (2017) Recent developments in joining of aluminum alloys. The Int J Adv Manuf Tech 91(5):1851–1866. https://doi.org/10.1007/s00170-016-9861-0
2. Çam G (2011) Friction stir welded structural materials: beyond Al-alloys. Int Mater Rev 56(1):1–48. https://doi.org/10.1179/095066010X12777205875750
3. Çam G, İpekoğlu G, Küçükömeroğlu T, Aktarer S (2017) Applicability of friction stir welding to steels. JAMME 2(80):65–85. https://doi.org/10.5604/01.3001.0010.2027
4. Schmidt H, Hattel J, Wert J (2004) An analytical model for the heat generation in friction stir welding. Model Simul Mater Sc 12(1):143–157. https://doi.org/10.1088/0965-0393/12/1/013
5. Vilaça P, Quintino L, dos Santos JF (2005) iSTIR—analytical thermal model for friction stir welding. J Mater Process Technol 169(3):452–465. https://doi.org/10.1016/j.jmatprotec.2004.12.016
6. Stewart M, Adams GP, Nunes Jr. AC, Romine P (1998) A combined experimental and analytical modeling approach to understanding friction stir-welding. NASA TechDoc. https://ntrs.nasa.gov/search.jsp?R=19990008766. Accessed 20 April 2017
7. J.E. Gould P. Ditzel 1996 Preliminary modeling of the friction stir-welding process. In: Conference on Joining of High Performance Materials, sponsored by ICAWT (International Conference on Advances in Welding Technology) Columbus, Ohio. p 297
8. Aziz SB, Dewan MW, Huggett DJ, Wahab MA, Okeil AM, Liao TW (2016) Impact of friction stir welding (FSW) process parameters on thermal modeling and heat generation of aluminum alloy joints. Acta Metall Sin-Engl 29(9):869–883. https://doi.org/10.1007/s40195-016-0466-2
9. Neto DM, Neto P (2013) Numerical modeling of friction stir welding process: a literature review. Int J Adv Manuf Tech 65(1-4):115–126. https://doi.org/10.1007/s00170-012-4154-8
10. Solomatine D, See LM, Abrahart RJ (2008) Data-driven modelling: concepts, approaches and experiences. In: Abrahart RJ et al (eds) Practical hydroinformatics. Springer-Verlag, Heidelberg, pp 17–30. https://doi.org/10.1007/978-3-540-79881-1_2
11. Liu Y, Zhang Y (2015) Iterative local ANFIS-based human welder intelligence modeling and control in pipe GTAW process: a data-driven approach. IEEE-ASME T Mech 20(3):1079–1088. https://doi.org/10.1109/TMECH.2014.2363050
12. Casalino G, Campanelli SL, Minutolo FMC (2013) Neuro-Fuzzy model for the prediction and classification of the fused zone levels of imperfections in Ti6Al4V alloy butt weld. Adv Mater Sci Eng 2013:1–7. https://doi.org/10.1155/2013/952690
13. Liao TW (2009) Improving the accuracy of computer-aided radiographic weld inspection by feature selection. NDT & E International 42(4):229–239. https://doi.org/10.1016/j.ndteint.2008.11.002
14. Liao TW, Li DM (1997) Two manufacturing applications of the fuzzy K-NN algorithm. Fuzzy Sets Syst 92(3):289–303
15. Liao TW (2003) Classification of welding flaw types with fuzzy expert systems. Expert Syst Appl 25(1):101–111. https://doi.org/10.1016/S0957-4174(03)00010-1
16. Gao XD, Wen Q, Katayama S (2013) Analysis of high-power disk laser welding stability based on classification of plume and spatter characteristics. T Nonferr Metal Soc 23(12):3748–3757. https://doi.org/10.1016/S1003-6326(13)62925-8
17. You D, Gao X, Katayama S (2016) Data-driven based analyzing and modeling of MIMO laser welding process by integration of six advanced sensors. Int J Adv Manuf Tech 82(5):1127–1139. https://doi.org/10.1007/s00170-015-7455-x
18. Martin O, Pereda M, Santos JI, Galan JM (2014) Assessment of resistance spot welding quality based on ultrasonic testing and tree-based techniques. J Mater Process Technol 214(11):2478–2487. https://doi.org/10.1016/j.jmatprotec.2014.05.021
19. Gao XD, Liu GQ (2015) Elucidation of metallic plume and spatter characteristics based on SVM during high-power disk laser welding. Plasma Sci Technol 17(1):32–36. https://doi.org/10.1088/1009-0630/17/1/07
20. Zhang ZF, Chen HB, Xu YL, Zhong JY, Lv N, Chen SB (2015) Multisensor-based real-time quality monitoring by means of feature extraction, selection and modeling for Al alloy in arc welding. Mech Syst Signal Pr 60-61:151–165. https://doi.org/10.1016/j.ymssp.2014.12.021
21. Yu J (2015) Quality estimation of resistance spot weld based on logistic regression analysis of welding power signal. Int J Precis Eng Manuf 16(13):2655–2663. https://doi.org/10.1007/s12541-015-0340-6
22. Dewan MW, Huggett DJ, Warren Liao T, Wahab MA, Okeil AM (2016) Prediction of tensile strength of friction stir weld joints with adaptive neuro-fuzzy inference system (ANFIS) and neural network. Mater Design 92:288–299. https://doi.org/10.1016/j.matdes.2015.12.005
23. Boldsaikhan E, Corwin EM, Logar AM, Arbegast WJ (2011) The use of neural network and discrete Fourier transform for real-time evaluation of friction stir welding. App Soft Comput 11(8):4839–4846. https://doi.org/10.1016/j.asoc.2011.06.017

24. Das B, Pal S, Bag S (2017) Weld quality prediction in friction stir welding using wavelet analysis. Int J Adv Manuf Tech 89(1):711–725. https://doi.org/10.1007/s00170-016-9140-0
25. Zhang Q, Mahfouf M, Panoutsos G, Beamish K, Norris I (2011) Multiple characterisation modelling of friction stir welding using a genetic multi-objective data-driven fuzzy modelling approach. In: Fuzzy Systems (FUZZ) IEEE International Conference pp 2288–2295. https://doi.org/10.1109/FUZZY.2011.6007731
26. Bhat NN, Kumari K, Dutta S, Pal SK, Pal S (2015) Friction stir weld classification by applying wavelet analysis and support vector machine on weld surface images. J Manuf Process 20(1):274–281. https://doi.org/10.1016/j.jmapro.2015.07.002
27. Das B, Pal S, Bag S (2017) Torque based defect detection and weld quality modelling in friction stir welding process. J Manuf Process 27:8–17. https://doi.org/10.1016/j.jmapro.2017.03.012
28. De Filippis LAC, Serio LM, Facchini F, Mummolo G, Ludovico AD (2016) Prediction of the vickers microhardness and ultimate tensile strength of AA5754 H111 friction stir welding butt joints using artificial neural network. Materials 9(11):915. https://doi.org/10.3390/ma9110915
29. Baraka A, Panoutsos G, Cater S (2015) A real-time quality monitoring framework for steel friction stir welding using computational intelligence. J Manuf Process 20:137–148. https://doi.org/10.1016/j.jmapro.2015.09.001
30. Bozkurt Y, Kentli A, Uzun H, Salman S (2012) Experimental investigation and prediction of mechanical properties of friction stir welded aluminium metal matrix composite plates. Mater Sci-Medzg 18(4):336–340
31. Das B, Bag S, Pal S (2017) Probing weld quality monitoring in friction stir welding through characterization of signals by fractal theory. J Mech Sci Technol 31(5):2459–2465. https://doi.org/10.1007/s12206-017-0444-2
32. Das B, Pal S, Bag S (2016) Monitoring of friction stir welding process using weld image information. Sci Tecnol Weld Joi 21(4):317–324. https://doi.org/10.1080/13621718.2015.1109805
33. Kumar U, Yadav I, Kumari S, Kumari K, Ranjan N, Kesharwani RK, Jain R, Kumar S, Pal S, Chakravarty D, Pal SK (2015) Defect identification in friction stir welding using discrete wavelet analysis. Adv Eng Softw 85:43–50. https://doi.org/10.1016/j.advengsoft.2015.02.001
34. Das B, Bag S, Pal S (2016) Defect detection in friction stir welding process through characterization of signals by fractal dimension. Manuf Letter 7:6–10. https://doi.org/10.1016/j.mfglet.2015.11.006
35. Soundararajan V, Atharifar H, Kovacevic R (2006) Monitoring and processing the acoustic emission signals from the friction-stir-welding process. P I Mech Eng B-J Eng 220(10):1673–1685. https://doi.org/10.1243/09544054JEM586
36. Teimouri R, Baseri H (2015) Forward and backward predictions of the friction stir welding parameters using fuzzy-artificial bee colony-imperialist competitive algorithm systems. J Intell Manuf 26(2):307–319. https://doi.org/10.1007/s10845-013-0784-4
37. Huggett DJ, Wahab MA, Okeil A, Liao TW (2017) On-line detection of friction stir welded joints by high temperature phased array ultrasonic inspection and control of weld process parameters. In: ASME 2017 12th International Manufacturing Science and Engineering Conference collocated with the JSME/ASME 2017 6th International Conference on Materials and Processing Los Angeles, California. V001T02A002. https://doi.org/10.1115/MSEC2017-2692
38. Huggett DJ, Dewan MW, Wahab MA, Okeil A, Liao TW (2016) Phased array ultrasonic testing for post-weld and on-line detection of friction stir welding defects. Res Nondestruct Eval 28(4):187–210. http://dx.doi.org/10.1080/09349847.2016.1157660
39. Roberts J (2016) Weld quality classification from sensory signatures in friction-stir-welding (FSW) using discrete wavelet transform and advanced metaheuristic techniques. Dissertation, Louisiana State University
40. Liao TW, Daftardar S (2009) Model based optimisation of friction stir welding processes. Sci Technol Weld Joi 14(5):426–435. https://doi.org/10.1179/136217109X425847
41. Murugananth M (2009) Metaheuristic multiobjective optimization in steel welds. Mater Manu Prosscess 24(2):230–239. https://doi.org/10.1080/10426910802612429
42. Karaboga D (2005) An idea based on honey bee swarm for numerical optimization. Tech. Rep.-TR06 Erciyes University. http://mf.erciyes.edu.tr/abc/pub/tr06_2005.pdf. Accessed 10 July 2017
43. Schiezaro M, Pedrini H (2013) Data feature selection based on artificial bee colony algorithm. EURASIP J Image Vide 2013:47. https://doi.org/10.1186/1687-5281-2013–47
44. Uzer M, Yilmaz N, Inan O (2013) Feature selection method based on artificial bee colony algorithm and support vector machines for medical datasets classification. Sci World J 2013. https://doi.org/10.1155/2013/419187
45. Shokouhifar M, Sabet S (2010) A hybrid approach for effective feature selection using neural networks and artificial bee colony optimization. In: The 3rd International Conference on Machine Vision Hong Kong, China. pp 502–506. https//doi.org/10.13140/2.1.2735.1045
46. Yavuz G, Aydin D (2016) Angle modulated artificial bee colony algorithms for feature selection. Appl Comput Intel Soft Computing 2016. https://doi.org/10.1155/2016/9569161
47. Prasartvit T, Banharnsakun A, Kaewkamnerdpong B, Achalakul T (2013) Reducing bioinformatics data dimension with ABC-kNN. Neurocomputing 116:367–381. https://doi.org/10.1016/j.neucom.2012.01.045
48. Karaboga D, Basturk B (2007) A powerful and efficient algorithm for numerical function optimization: artificial bee colony (ABC) algorithm. J Glob Optim 39(3):459–471. https://doi.org/10.1007/s10898-007-9149-x
49. Wong T-T (2015) Performance evaluation of classification algorithms by k-fold and leave-one-out cross validation. Pattern Recogn 48(9):2839–2846. https://doi.org/10.1016/j.patcog.2015.03.009